

Chapter 4

Design and Modeling of a Novel Exoskeleton Suit for Load-Bearing Augmentation



Shivansh Mishra, Jyotindra Narayan, Ankit Kumar Nikum, and Rajat Singh

1 Introduction

An exoskeleton is a structure with actuators (electric, hydraulic, and pneumatic) controlled by an electronic circuit to assist in physical work (Toxiri et al. 2018) and locomotion of the wearer (Gorgey et al. 2019). Exoskeletons are famous nowadays as rehabilitation devices in therapeutic medicine (Narayan et al. 2021) and load-augmentation devices within different industrial sectors (Toxiri et al. 2018). In case of post-stroke and spinal cord injury (SCI), the exoskeleton assists the patients to regain motor strength and provides better social life by performing different activities of daily living (ADLs). Moreover, the harmful consequences of increased sitting time on cardiovascular health can be revamped by using exoskeleton devices at the expense of physical activity (Gorgey 2018). Although people with neurological disorders use either a stick or wheelchair for locomotion, they cannot assist specific tasks like natural walking and climbing stairs without an exoskeleton device (Dhand et al. 2016). Narayan et al. (2020) designed a wheelchair-based sit-to-stand exoskeleton (STSWE) model for paraplegic children. This wheelchair exoskeleton can turn into an exoskeleton when needed, with the help of gear and a dog-clutch mechanism. The basis of the design is to verify the dynamic analysis for different subjects at seat-off position using a neural network approach. On the other hand, industrial workers who perform manual handling of heavy loads through stoops and turns have an increased risk of musculoskeletal problems (Ratti and Pilling 1997). These problems can be reduced with the help of load-augmenting exoskeletons. Moreover, exoskeletons can also be used as lumbar distraction devices to reduce pressure in the intervertebral

S. Mishra · A. K. Nikum · R. Singh
Department of Mechanical Engineering, Sardar Vallabhbhai National Institute of Technology,
Surat 395007, India

J. Narayan (✉)
Department of Mechanical Engineering, Indian Institute of Technology Guwahati, Assam 781039,
India

disk in the lower spine. Lumbar traction is a physical therapy procedure used to treat lower back pain by lessening the mechanical stress on the lower back (Zaïri et al. 2021).

Based on human body mechanics, exoskeletons can be classified into three categories—upper body, lower body, and full body exoskeleton. The upper body exoskeleton augments the strength and assists the movement of the wearer's arm (Narayan et al. 2021). These can be classified based on the joint or part of the arm they assist—shoulder (Kiguchi et al. 2003), elbow (Hosseini et al. 2017), forearm (Kung et al. 2007), wrist (Pang et al. 2020), and finger (Nilsson et al. 2012). The upper body exoskeleton can also assist a combination of arm segments—shoulder-elbow (eksoBIONICS 2021; Kim et al. 2018; Pedrocchi et al. 2013), shoulder-elbow-forearm (Rahman et al. 2012), and shoulder-elbow-forearm-wrist (Yan et al. 2021; Kazerooni and Guo 1993). The lower body exoskeleton augments and assists the movement of the lower leg. They can be classified based on the assistance to the anthropometric portion of the body (hip, knee, ankle, and their combination) (Kalita et al. 2020). BLEEX (Zoss et al. 2006) and MIT exoskeleton (Walsh et al. 2007) are lower body exoskeleton which assists trunk, hip, knee, and ankle joints. HAL-5 (Sankai 2010), Walking Power Assist Leg (WPAL) (Chen et al. 2007), and a pediatric lower limb exoskeleton system (Narayan and Kumar Dwivedy 2021) assist hip, knee, and ankle joints. Exoskeleton for Patients and The Old by The Sogang University (EXPOS) (Kong and Jeon 2006) and ABLE (Mori et al. 2006) are designed and developed to assist hip joint and knee joint. There are lower body exoskeletons that assist only a single joint, viz., robotic hip exoskeleton (for hip) (Junius et al. 2017; Seo et al. 2017) and RoboKnee (for knee) (Pratt et al. 2004). A full body exoskeleton can be defined as a hybrid arrangement having features of both upper and lower body exoskeletons (Dhand et al. 2016; Fontana et al. 2014; Christensen et al. 2018). The major fraction of load is transferred from its upper body to the lower body via exoskeleton joints and, eventually, to the ground (Mattsson et al. 2018). Full body exoskeletons are basically wearable suits whose joints are aligned with the wearer's joint and structure is parallel to the wearer's body.

On the other hand, the exoskeleton can be further categorized into load-augmentation exoskeleton and rehabilitation exoskeleton based on the application. Load-augmentation exoskeletons enhance the strength of a person while lifting and carrying heavy objects for several hours (Zaïri et al. 2021; Nilsson et al. 2012; eksoBIONICS 2021; Kim et al. 2018; Zoss et al. 2006; Walsh et al. 2007; Sankai 2010; Fontana et al. 2014; Christensen et al. 2018; Mattsson et al. 2018; Martinez et al. 2007). Load-augmentation exoskeletons reduce the force and frequency of the force exerted by the load on the wearer. These are effective in industries where heavy objects are maneuvered by the workers, like the automobile industry, aircraft manufacturing, and maintenance industry. On the contrary, rehabilitation exoskeletons enable the user to perform daily locomotion tasks independently and offer therapy after trauma (Kung et al. 2007; Nilsson et al. 2012; Pedrocchi et al. 2013; Rahman et al. 2012; Narayan and Kumar Dwivedy 2021; Kong and Jeon 2006; Mori et al. 2006; Junius et al. 2017; Seo et al. 2017; Pratt et al. 2004). The literature in this work is limited to the design implementation of load-augmentation exoskeletons.

Upper body exoskeleton devices for load-augmentation purposes are Ekso Vest (eksoBIONICS 2021; Kim et al. 2018), SEM Gloves (Nilsson et al. 2012), Human extenders (Kazerooni and Guo 1993), and Intelligent Assist Device (IAD) (Martinez et al. 2007). Ekso Vest, developed by Ekso Bionics (eksoBIONICS 2021), is a passive upper body exoskeleton for assistance in overhead industrial works. It contains a moment generation and a hinge mechanism that reduces the wearer's fatigue to endure the tools' weight for an extended duration (Kim et al. 2018). Developed by BioServo, SEM Gloves (Nilsson et al. 2012) is an upper body exoskeleton that assists the wearer in grasping objects by sensing the force applied and providing feedback to the actuator. It has a fabric glove with strong Bowden cables to serve as artificial tendons and is controlled by actuators inside a backpack having a battery. The exoskeleton weighs 700 gm and can generate 3–4 N force at the fingers to augment the force of the wearer. Human extenders (Kazerooni and Guo 1993) is a 6-DOFs upper body exoskeleton developed at the University of California in Berkeley. It is operated by hydraulic actuators, controlled by the generated contact force signals between the exoskeleton and the wearer's arm. A device of a non-wearable kind, Intelligent Assist Device (IAD) (Martinez et al. 2007), is designed as a simple upper body exoskeleton to augment the load transfer capabilities using a fractional form of weights via sensors and cables.

In case of lower body, the well-known load-augmenting exoskeletons are BLEEX (Zoss et al. 2006), MIT exoskeleton (Walsh et al. 2007), HAL-5 (Sankai 2010), and treadmill-based lower body exoskeleton (Tagliamonte et al. 2013). BLEEX (Zoss et al. 2006) is a 7-DOFs lower body exoskeleton (three at hip, one at knee, and one at ankle) with the characteristic feature of portability and generating high power. The hydraulic actuators are utilized to generate high force and amplify the human capacity while carrying a heavy load. Another load-supplementing exoskeleton, developed at MIT (Walsh et al. 2007), has 6 DOFs, two at the hip, two at the knee, and two at the ankle. It can generate 130 Nm at the hip, 50 Nm at the knee, and 90 Nm at the ankle. Hybrid Assistive Leg (HAL-5) load-augmentation and rehabilitation device (Sankai 2010), designed by Cyberdyne (University of Tsukuba, Japan), enables the user to augment the load up to 70 kg. It has an operating time of 160 min. The treadmill-based exoskeleton, developed by Tagliamonte et al. (2013), exploits the 4-DOFs arrangement attached to the lower body—for hip f/e and for knee f/e at each leg. All four joints are actuated by compliant actuators (SEAs) in the sagittal plane. The compliant actuators provide 10 Nm back-driving torque and can be controlled to provide variable torque to ensure smooth operating conditions.

Karlin (2011), AXO-Suit (Christensen et al. 2018; Mattsson et al. 2018), and Body Extender (BE) (Fontana et al. 2014) and Modular Agile eXoskeleton (MAX) (SuitX 2021) are the well-known full body exoskeletons for load amplification. Sarcos (Karlin 2011) is a full body exoskeleton with rotary hydraulic actuators, enabling the wearer to walk at 1.6 m/s while lifting 70 kg of load. AXO-suit (Christensen et al. 2018) is a full body exoskeleton for assisting the elderly with locomotion and performing medium-load intensive day-to-day tasks. It is divided into upper body and lower body modules with 27 DOFs, 15 DOFs (3 at spine, 6 at each arm) in the upper body module, and 12 DOFs (6 at each leg) in the lower body

module. It provides the strength to lift and carry a 5 kg load in each arm for an hour (Mattsson et al. 2018). The body extender (BE) (Fontana et al. 2014), developed by the PERCRO laboratory, TeCIP Institute, is another full body exoskeleton for load-bearing purposes. It has 22 DOFs, 6 DOFs at each leg and 5 DOFs at each arm, all powered by electric actuators. It is a heavy exoskeleton weighing 160 kg and carrying up to 100 kg load at 0.5 m/s walking speed. Modular Agile eXoskeleton (MAX) (SuitX 2021), developed by SuitX, a US company, is a modular full body exoskeleton consisting of BackX, LegX, and ShoulderX. BackX is a passive upper body exoskeleton that reduces lower back muscle forces while lifting load. LegX provides support in the tasks which require squatting for a long time in industries. ShoulderX provides support to the shoulder and arms of the wearer carrying tools and load in overhead tasks.

It is evident from the literature that there are only a few full body exoskeletons available for load-augmentation purposes. Moreover, the design criteria of such exoskeletons are yet to be explored extensively. Therefore, in this work, the design and modeling of a novel full body exoskeleton are proposed for weight carrying capacity. Table 1 presents a vis-a-vis comparison of novel design features for different load-augmentation exoskeleton devices and the full body exoskeleton proposed in this work.

The above state of comparison demonstrates that the proposed exoskeleton design amalgamates several original features such as.

- Lightweight, as it is fabricated using rectangular hollow cross section of Aluminium 1060 alloy having high strength-to-weight ratio. Further, passive joints in the lower body module make it more lighter.
- Portability, the exoskeleton has on-board power source and therefore can be carried from one place to another easily.
- Low complexity, the number of DOFs provided is reduced to 12 (4 active and 8 passive) keeping the DOFs restricted from movement to avoid complex configuration of the exoskeleton.
- Optimized structure, iterative development of the exoskeleton structure was done with focus on wearer comfort while lifting and carrying the load.
- Active–passive actuation, a combination of active (linear actuators at shoulder and elbow joint) and passive actuators (gas springs at knee joint) are selected to optimize the duty cycle.

Furthermore, the proposed design has promising advantages as follows:

- The proposed exoskeleton design comprises upper body as well as lower body module which efficiently transfers load to the ground.
- Passive joints in the lower body module increase the duty cycle.
- The design dimensions are focused to serve the young industry workers of the country.

Firstly, the methodology for a general exoskeleton design is explained based on the literature. Thereafter, the design and development of a full body load-augmenting

Table 1 Vis-a-vis comparison between load-augmentation exoskeletons and proposed exoskeleton

Exoskeleton	Developer	Design feature
Ekso Vest (eksoBIONICS 2021; Kim et al. 2018)	Ekso Bionics	Passive spring loaded mechanism to support load
Human Extenders (Kazerooni and Guo 1993)	University of California, Berkeley	Extender hands to grasp heavy loads, contact force of wearer control the actuators using sensors
SEM Gloves (Nilsson et al. 2012)	BioServo	Tendon-like actuators, under-actuated fingers
Intelligent Assist Device (IAD) (Martinez et al. 2007)	University of California, Berkeley	Simplest industrial load-augmentation device, non-anthropomorphic, uses wire ropes, and suction cup/hook
BLEEX (Zoss et al. 2006)	University of California, Berkeley	Higher load capacity and rotary joints
MIT Exoskeleton (Walsh et al. 2007)	MIT	Passive spring (hip, ankle) and damper (knee) mechanism
HAL-5 (Sankai 2010)	Cyberdyne (University of Tsukuba, Japan)	<ul style="list-style-type: none"> • Application for load augmentation as well as rehabilitation • Bio-electrical signals on skin's surface
Sarcos (Karlin 2011)	Raytheon Sarcos	Application in military missions, heavy though agile
Body Extenders (Fontana et al. 2014)	PERCRO laboratory, TeCIP Institute	Pantograph mechanism and pulley-based actuator for wide range of motion with high torque
Modular Agile eXoskeleton (MAX) (SuitX 2021)	SuitX	Modular, customizable, supports the wearer by reducing exertion, fatigue
Proposed Full Body Exoskeleton (in this work)	SVNIT Surat and IIT Guwahati	<ul style="list-style-type: none"> • Linear actuators (at shoulder and elbow joints) • Industrial load-augmentation device, no ceiling setup required, • Passive gas springs (damper) (knee) and four-bar mechanism for better stability

exoskeleton are described in detail using the CAD model. The finite element analysis of the critical components is carried out for different conditions. Finally, the corresponding stress and deformation results are carried out in a detailed manner. The organization of the remaining chapter is given as follows. In Sect. 2, design methodology and CAD modeling are presented. Section 3 explains the details of the FEA analysis. The related results are discussed in Sect. 4. The future directions are pointed out with the concluding remarks of the complete work in Sect. 5.

2 Design and Modeling of Full Body Exoskeleton System

The design methodology and modeling of the full body exoskeleton based on the design process are presented in this section. At first, the methodology is explained in different stages, starting from the design statement and ending at complete prototype development. Thereafter, in the subsequent subsection, the CAD model of the proposed full body exoskeleton system is presented with the details of mechanical and electric modules.

2.1 Design Methodology

The complete design process can be divided into five stages, as shown in Fig. 1. Stage 1 recognizes the problem by searching for need, deciding on the device category, and research for the prerequisites. The research includes the clinical and technical study of the recent similar devices and technologies used. The output of this stage is the documentation based on the device category and to be used in further stages. Stage 2 is the proper presentation of the idea after defining mechanical modules with dimensions, connections, DOFs, and electronic modules with the circuit, referring to the documentation. The output is a conceptual design of the exoskeleton/device. Therefore, Stage 3 is the realization of the design by making CAD modules and integrating mechanical modules, actuators, and electronic modules into an assembly. Stage 4 presents the simulation of the CAD assembly using documentation made earlier, which generates a database for evaluating the prototype. This database can be used to assess and modify the prototype (physical model) for ranges of motion and

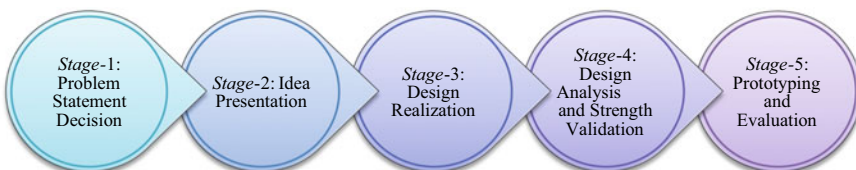


Fig. 1 Proposed methodology

mechanical failure during movement. Moreover, the design strength and analysis with a different set of boundary conditions is computed. In Stage 5, the prototyping and appropriate material selection based on strength analysis can be considered. Finally, the evaluation of the developed prototype could be performed to make decisions for future directions. For that, a survey could be carried out in the recreated or original workplace environment in the presence of experts and take feedback from them over design criteria as discussed in the literature (Rubin and Chisnell 2008). This type of survey helps to develop a statistics-based performance index of the device, which helps in the future development of the device.

This design methodology is followed up to Stage 4 for the exoskeleton design and analysis. Therefore, this work covers only computer-aided design of the mechanical modules and the finite element-based strength analysis of critical submodules. In the following subsection, the proposed design and modeling of the full body exoskeleton are presented.

2.2 Proposed Design of Exoskeleton

The device was designed considering the needs of automotive industries and manufacturing industries near the lab. A survey was conducted to determine dimensions and capacity of the exoskeleton in the industries near the lab. For that, male industrial workers of age ranging 22–28 years old (height: 5'6"–6'0") are selected. The workers of the industries were found to frequently lift and carry heavy loads of 50 kg. Consequently, they faced health issues related to back pain and fatigue. Therefore, we decided to conceive a device to relieve industry workers from lower back muscle injury by reducing the force sustained by the arm muscles. At first, (Stage 1) the state of the art used for the exoskeleton is of armor or mechanical suit to assist back [48], shoulder/arm (Kim et al. 2018), and legs [49], which can be attached to the wearer's body using straps, cuffs, or held via the handle at the hands. The shoulder, elbow, hip, knee, and ankle joints at all limbs are kept revolute joints, capturing their f/e movements. Actuator technologies for existing exoskeleton devices were studied, and electrical actuators are found suitable for their compactness, load capacity, and power source availability. The concepts of ergonomics and biomechanics of shoulder and elbow joints were studied. Similarly, other design criteria were also decided based on the design, engineering, and application gaps in the existing exoskeleton, which are presented in the Table 2. Based on the limitations, the current full body exoskeleton is designed in following stages.

Thereafter, (Stage 2), taking average of the body dimensions from the survey, the dimensions of the proposed exoskeleton design are selected according to a 5'10" healthy male. The shoulder and elbow joints for f/e movements are kept active for load augmentation, while hip, knee, and ankle joints for f/e movements are kept passive for power-saving features. The motion of the wrist supporting the forearm, shoulder joint's abduction/adduction (a/d), and the hip joint's abduction/adduction (a/d) movement are restricted. The restrictions ensured the stability of the system and

Table 2 Comparison among existing load-augmentation exoskeleton for industry needs

Exoskeleton	Description	Load capacity	Application	Limitation
EksoVest (eksoBIONIC 2021; Kim et al. 2018)	Spring-loaded mechanism, reduces fatigue, increases productivity	2.2–6.8 kg	Load lifting in warehouses, also overhead jobs in manufacturing industries and construction work	No active joints for load lifting and carrying has no support for lower body
Human Extenders (Kazerooni and Guo 1993)	6 DOFs, hydraulic actuators, direct driven, controlled using contact force signals	227 kg	Handling of heavy objects	Portability, space constraints due to hydraulic actuators
Intelligent Assist Device (IAD) (Martinez et al. 2007)	Ropes and electric actuators, simple, non-wearable	27–32 kg	Handling of parts in assembly lines in automotive industries, loading–unloading of trucks in warehouses and distribution centers	Large space, ceiling setup requirements, safety issues with possibility of slack in rope
BLEEX (Zoss et al. 2006)	7 DOFs, hydraulic actuators, Portability, high power generation	34 kg	Carrying food, rescue equipment, in rescue operations and weapons in military missions	No support to lift load in hands (upper body), high power consumption, heavy weight (75 kg including payload)
MIT Exoskeleton (Walsh et al. 2007)	6 DOFs, Spring-loaded mechanism (hip, ankle) and damper (knee), quasi-passive	36 kg	Carrying heavy loads on back in military missions, industries	No support to lift load in hands (upper body), does not bears load directly, only supports the wearer
HAL-5 (Sankai 2010)	Electric actuators, High load capacity	70 kg	Carrying heavy loads in industries, hospitals, rescue missions	High price, not affordable by small-scale industries
Sarcos (Karlin 2011)	Rotary hydraulic actuators, High load capacity, power efficient	70 kg	Carrying heavy loads in military missions	Heavy weight (90 kg), tethered power source

(continued)

Table 2 (continued)

Exoskeleton	Description	Load capacity	Application	Limitation
Body Extenders (Fontana et al. 2014)	22 DOFs, Electric actuators, High load capacity, heavy weight (160 kg)	100 kg	Carrying, handling of heavy objects	Requiring sufficient training to operate, slow speed, difficulty in handling objects
Modular Agile eXoskeleton (MAX) (SuitX 2021)	Modular, passive, lightweight (3.17 kg), customizable	~15–20 kg	Overhead tasks in industries	Does not bears load directly, only assists the wearer

avoided the complex movements in the exoskeleton. Moreover, the alignment of the exoskeleton joints with the body joints is considered, to the maximum possible extent, for the physiological safety of the user. Ergonomic factors are considered while attaching the user’s body to the exoskeleton. Straps are provided at the shoulders, waist, thigh, and lower leg, and the back frame is cushioned.

As shown in Fig. 2a, b of the exoskeleton, the conceptual design is 12 DOFs, having 3 DOFs each for every upper arm and lower limb. In the upper limb, a 2-DOFs active–passive arrangement is made at the shoulder joint for f/e and i/e movements, and a 1-DOF linear-actuated mechanism is kept at the elbow joint for f/e movements. On the other hand, all 3 DOFs are kept passive for f/e movement of the hip, knee, and ankle joint in the lower limb. As explained earlier, only 12 DOFs are provided in the design to lessen the complexity of motion and for augmenting

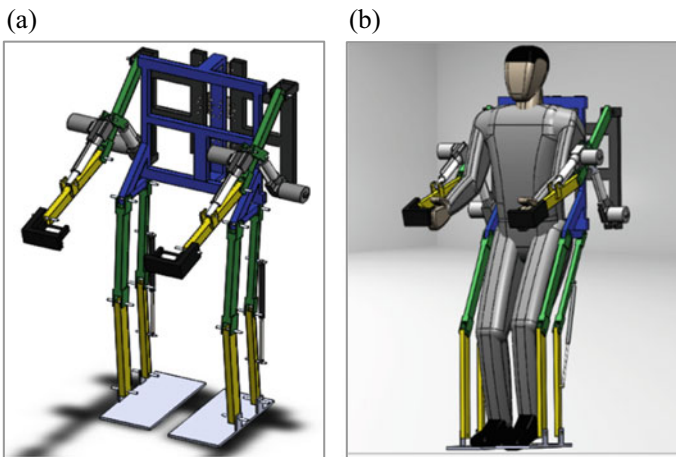


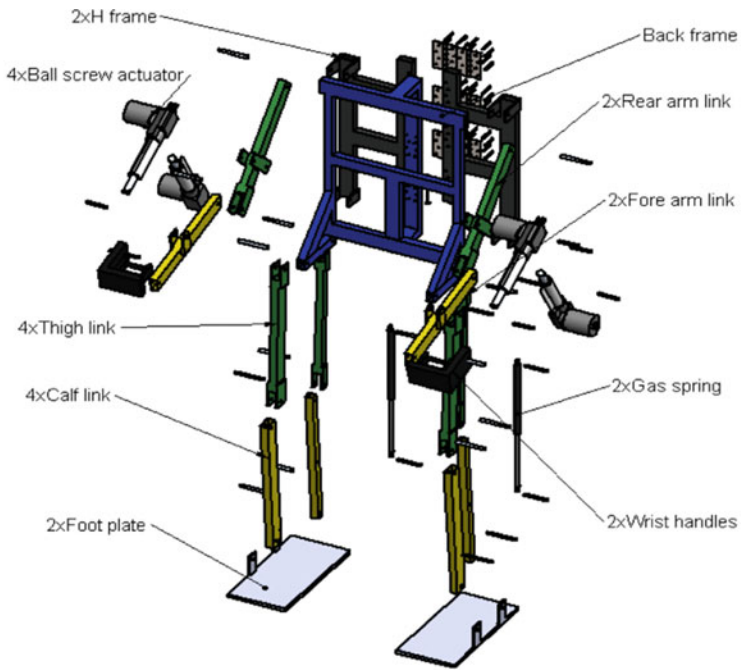
Fig. 2 Conceptual view of the proposed design **a** isometric view of the proposed design; **b** isometric view with a human dummy

the physiological safety of the user. For active joints, a linear actuator with a load capacity of 3000 N is designed at each shoulder (between the Scapula and upper arm) and each elbow (between the rear arm and forearm). Two gas springs of 20 KN/m stiffness are exploited and appended between the thigh and calf for the passive joints at the knee. Aluminium shafts of 10 mm diameter are used at the joints for revolute movement. For the i/e movement with a passive joint at the shoulder, stainless steel door hinges with holes of 6 mm diameter are used. All the joints are aligned with the wearer's joint except the passive joint of the shoulder, which is kept behind the back frame with the axis at the spine for structural rigidity and stability. A handle with a control panel and load-lifting hooks is given at the wrist to actuate the exoskeleton. The control unit (circuit of microcontrollers) and power unit (battery) are provided near the back frame.

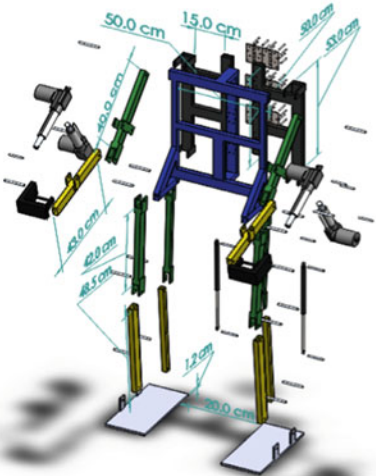
Now (Stage 3), the realization of the exoskeleton is done by dividing it into two modules, mechanical and electronic. The mechanical module consists of arm links (forearm links, rear arm links, wrist handle), double H-frame (two H-frames supporting Scapula), back frame (back section, spine base, and waist support), and leg links (thigh links, calf links). On the other hand, the electronic module comprises actuators, buck converter, motor driver, control switches, and Li-Po battery. In this work, the mechanical submodules are presented extensively; however, only important ones in the case of the electronic module.

The CAD modeling of the proposed design is carried out using SolidWorks software. The exploded view of the exoskeleton in trimetric view is shown in Fig. 3a and the components' dimensions are shown in Fig. 3b, c. The total weight of the exoskeleton is 15.71 kg (including actuator and springs) as computed from the SolidWorks. An aluminium cuboid with a hollow rectangular cross-sectional area of $50 \times 25.4 \times 2 \text{ mm}^3$ is selected for designing all links. The orientation of the cross section of links is used strategically to increase the structure's performance in bending. As shown in Fig. 3b, for the forearm links, a cuboid of length 43 cm is considered on each side. Moving from the elbow joint toward the forearm and rear arm, the extrusions are designed at the distance of 22.5 and 15.5 cm to hinge the linear actuator. The rear arm link at each side is made up of a 40 cm length box section as shown in Fig. 3b. Each forearm and rear arm link weigh about 0.37 and 0.62 kg, respectively. C-type aluminium connector with 6 mm thickness is brazed at the proximal end of the rear arm and connected with the distal end of the forearm to construct the elbow joint. Two wrist handles, each of 0.61 kg, are designed to hold and control the actuators using a control switch. Figure 3b further indicates that each H-frame is a ladder-shaped structure with inner and outer vertical links of 50 and 53 cm in length and two horizontal links of 15 cm. The mass of each H-frame is 0.97 kg. On the outer vertical link, extrusions with 10 and 7.8 mm diameter holes are provided at the upper and lower ends to form the shoulder i/e joints and shoulder actuator hinges. The back frame, having a total mass of 2.85 kg, comprises three parts—the back section, spine base, and waist support. As shown in Fig. 3c, the back section is designed as a rectangular-shaped structure having dimensions of $50 \times 49 \text{ cm}^2$ and encloses a "T-shaped" arrangement. The spine base is planned with two horizontal links of 12.5 cm extruded backward and a vertical link of 59 cm. The spine base is

(a)



(b)



(c)

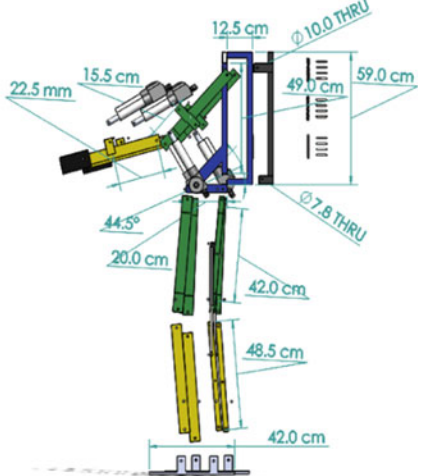


Fig. 3 Exploded model of proposed exoskeleton design with **a** submodules' names, **b** dimensions from trimetric view, and **c** dimensions from side view

provided to shift the center of mass (COM) of the exoskeleton at the plane of the back and reduces the toppling effect while loading. Waist support is made up of a horizontal link, and a slant link of length 20 cm protruded at the bottom of the back section. These are fastened at an angle of 44.5° to the back section, as shown in Fig. 3c.

Moving further to the lower body exoskeleton, both thigh and calf links for each leg are designed in the form of two distinct four-bar mechanisms. The length of thigh and calf links in the mechanism is selected as 42 and 48.5 cm, respectively, as shown in Fig. 3c. Two thigh links on one side of the exoskeleton leg weigh about 0.60 and 0.32 kg whereas the masses of two calf links on one side are 0.31 and 0.22 kg. Two C-type connectors with 6 mm thickness are brazed on both ends of the thigh link to form the hip and knee joint. Figure 3b, c shows that the foot is a rectangular plate of dimensions $42 \times 20 \times 1.2 \text{ cm}^3$ and mass 0.66 kg with two hook-like extrusions as ankle joints. Furthermore, all the mechanical submodules are integrated into an assembly along with the electronic submodules. For example, the ball screw linear actuators and gas springs, shown in Fig. 3, are designed to integrate with other electronic submodules such as buck converter, motor driver, ultrasonic sensors (at the wrist to provide data of height above the ground), control switches, and Li-Po battery. These submodules are evaluated for their parallel functioning, and several iterations are made for efficient design, which could eventually lead to the final prototype in the future.

3 Design Analysis: Boundary Conditions

The design analysis (stage 4) of different mechanical submodules of the exoskeleton is carried out in ANSYS structural workbench software. The aim of this analysis is to check the failure of the critical submodules in extreme loading conditions based on the stresses and deformation. The analysis built upon these extreme conditions ensures the safety of the components during various tasks. Although the effect of interaction between the components is taken into account using the help of appropriate force transfer, the analysis is performed part by part owing to the computation limits of the system used and to reduce the complexity of the problem. Reaction forces and moments are calculated by considering equilibrium conditions at every point of time; therefore, net torque and net forces put to zero in order to get the reaction forces and moments for every submodule. Magnitude and direction of calculated forces are shown in Figs. 4, 5, 6, 7 and 8. Stress generated by application of these forces on submodules must not exceed the yield strength of the material used for the design to work perfectly. In order to observe variation of stress along the whole dimensions of submodules, the end of the submodule needs to be fixed so that the load can be transferred to another submodule. The fixing of these ends is carried out using the “Fixtures” option in ANSYS structural analysis.

The submodules are imported to ANSYS structural workbench from SolidWorks as an IGS file. Four integrated submodules such as forearm link with wrist handle,

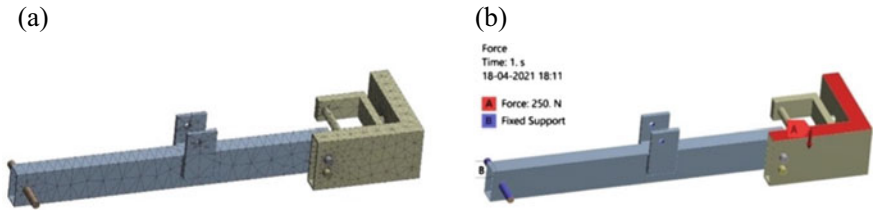


Fig. 4 a Mesh generation for forearm link; b Applied force and a fixed support

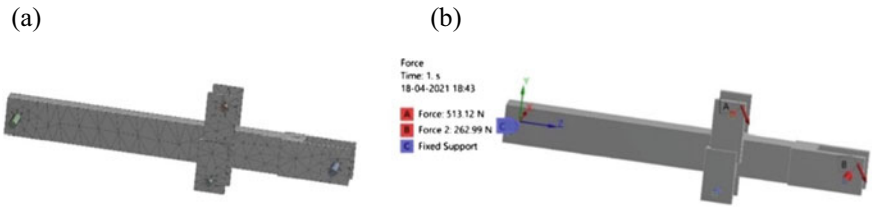


Fig. 5 a Mesh generation for rear arm link; b Applied forces and a fixed support

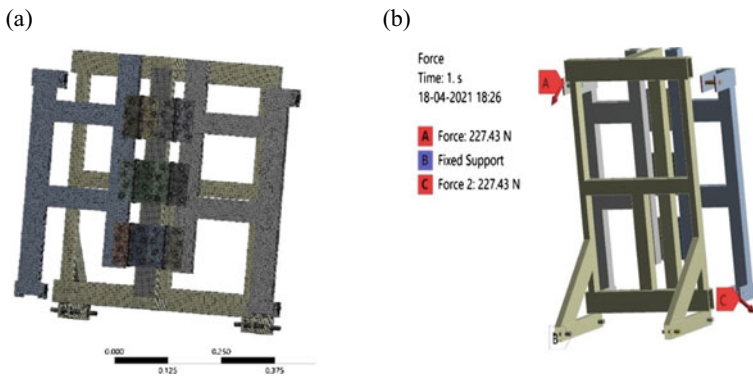


Fig. 6 a Mesh generation for double H-frame along with back frame; b Applied forces and a fixed support

rear arm link, double H-frame with the back frame, and leg links are considered critical submodules that bear significant stresses and lead to large deformations.

The forearm link and wrist handle are fastened using mild steel bolts. In the customization tab, mild steel as new material is added by referring to various standard property charts. Handles, links, and shafts are made up of an aluminium alloy 1060, and related properties are allocated in the material assignment. After assigning material to all the parts in a static-structural module, a mesh is generated in the forearm, as observed in Fig. 4a. Mesh sensitivity analysis was performed and solid elements (SOLID 187 and SOLID 186) provide better meshing results. The number of

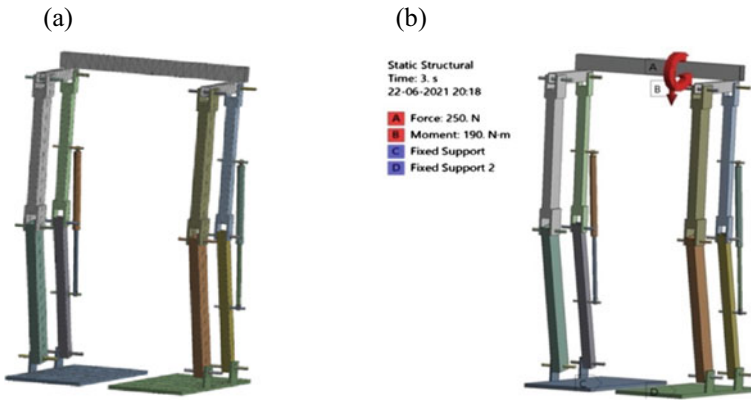


Fig. 7 When both feet are in ground contact **a** Mesh generation for leg links; **b** Applied force, moment, and fixed supports

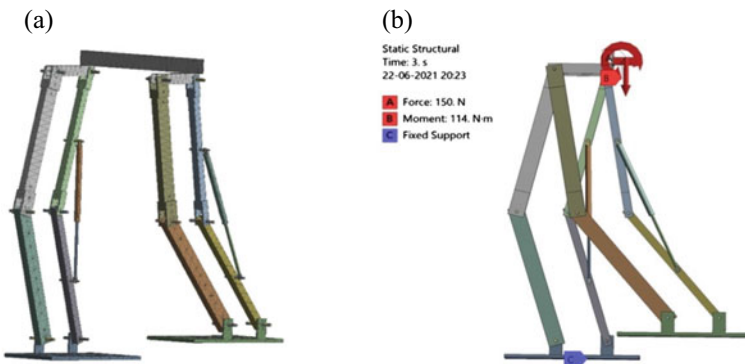


Fig. 8 When left leg swinging in the air **a** Mesh generation for leg links; **b** Applied force, moment, and fixed support

nodes for the forearm link and handle is 8021 and 5465, respectively. Corresponding number of elements (SOLID 187 and SOLID 186) for the forearm link and handle are 3947 and 2580. Additionally, number of nodes and elements (SOLID 186) for shafts are kept as 2289 and 448, respectively. As per the survey conducted in design Stage I, assuming the exoskeleton can lift 50 kg, a reaction force of 250 N downward is applied on the handle attached with each arm. The direction and magnitude of the force can be observed at point A in Fig. 4b. The rear shaft is kept as fixed support, shown at point B in Fig. 4b.

The force gets transferred from the forearm link to the rear arm link during the load lifting, making it one of the critical parts to analyze. As made up of aluminium alloy 1060, it is assigned the same material. A global coordinate system is declared for the structural analysis of the rear arm link. Figure 5a shows that the mesh is

generated with a number of nodes as 17,341 and elements (SOLID 187) as 5633 for the rear arm link. Number of nodes and elements (SOLID 186) of shafts is kept as 2551 and 501, respectively. The reactions are calculated at equilibrium conditions, i.e., by considering net force and net moment equals zero.

Conservation of forces in X-direction,

$$F_B^i + F_A^i + F_C^i + F_{ext}^i = 0 \quad (1)$$

Similarly, conservation of force in Y-direction,

$$F_B^j + F_A^j + F_C^j + F_{ext}^j = 0 \quad (2)$$

and conservation of momentum at point C,

$$l_2^i \times F_B^j + l_3^i \times F_A^j = 0 \quad (3)$$

F_A , F_B , and F_C are reaction forces at point A, B, and C, respectively, F_{ext} is 250 N, l_2 , l_3 , and l_1 are distance between BC, AC, and AB, respectively. The magnitude of the forces comes out to be 452.91 N at point A in the y-axis direction and 240.90 N at point A in the z-axis direction, making the resultant as 513 N. At point B, the respective forces in y- and z-directions are 227.53 N and 131.8 N, forming the resultant as 263 N. The reaction force at point A and B is shown in Fig. 5b. The rear shaft (at point C) shown in Fig. 5b is kept as fixed support.

Furthermore, the aluminium alloy is assigned to double H-frame and back frame in the material assignment. Three hinges made up of stainless steel are used to connect both H-frames. Forces are transferred from wrist handles to H-frames via arm links, and thereafter hinges start to perform the required movement. Therefore, hinges along with the H-frames and back frame are the critical components. Figure 6a shows mesh generation for double H-frame and back frame along with hinges. Respective number of nodes and elements (SOLID 187) for left and right H-frames are kept as 71,715 and 36,974, and 72,970 and 37,554. Moreover, the back frame has 21,276 nodes and 21,505 elements (SOLID 187). The magnitude of the force at points A and C is calculated using

$$\frac{(p \times e \times l_1)}{(2(l_1^2 + l_2^2))} \quad (4)$$

where l_1 and l_2 are the distances from the reference for points A and C, respectively.

The reference is considered passing from point C, making l_1 zero and l_2 equal to the length of the H-frame itself. The e is the perpendicular horizontal distance from the wrist handle to the back section, and p is the load applied at the wrist handle, as mentioned in Fig. 6b. This formula applies to bolts and rivets when there is an eccentric force application on the system. The final calculated force at both points

A and C is 227.43 N. The shafts connecting the lower exoskeleton to the upper ones through the waist are kept as fixtures. It can be observed as point B, as shown in Fig. 6b.

The leg link consists of the thigh link, calf link, hip joint, knee joint, and ankle joint. The material is assigned as aluminium alloy 1060 in ANSYS to all the parts. A few components, for instance, the bolts and the gas springs are originally made of different materials like MS and stainless steel; however, as both the materials have strength greater than aluminium alloy 1060 the results hold valid. Both the thigh link and calf link are made of two separate links in parallel. There are a total of 12 revolute joints in the assembly. A revolute joint is originally the connection of two links with a shaft; however, in the analysis, all the revolute joints are assigned a bonded contact with the respective links for simplifying the system and making the whole system a rigid body. The rigid contact can be assumed as a weld between the joints; however, as the stresses within the region of the joint are of prime importance, the assumption does not significantly affect the results. The static-structural analysis for the submodule is done for two conditions: first, when both feet are on the ground (Fig. 7) and second when the left foot is swinging in the air (Fig. 8). The first condition depicts the situation of holding the load in a static state and the second situation can be considered as an instant when the subject is walking while lifting the load. A more reasonable approach for analyzing the second situation is to perform the dynamic analysis, which is carried out in future work. The automatic mesh option is used to carry out analysis for both conditions. As shown in Figs. 7a and 8a, the generated mesh comprises triangular elements (SOLID 187). The total number of nodes and elements are kept as 37,304 and 13,841, respectively.

The direction of the forces transferred from the upper body exoskeleton to the lower one is shown in Figs. 7b and 8b. Although the point of application of force and moment in both conditions is similar, the magnitude differs according to different walking instants. For the first case, both the legs are on the ground; therefore, both feet are defined as fixed support (at points C and D in Fig. 7b). On the other hand, for the second condition, the left leg is in the air, and only the right foot is fixed (at point C in Fig. 8b). A downward force of 250 N (at point A) is applied on the center of the horizontal spine link, and a moment of 190 Nm (at point B) is applied about the side faces on the center of the link, as shown in Fig. 7b for the first case. The second case is considered an instant dynamic condition where the load on left leg links decreases approximately 60% (Narayan and Kumar Dwivedy 2021). Therefore, a downward force of 150 N (at point A) and a moment of 114 Nm (at point B) are applied to the center of the horizontal spine link, as shown in Fig. 8b. The loading conditions are decided by using simple Newtonian mechanics. The downward force is applied to replicate the transfer of load lifted with the hand assembly which then transfers the load to the rib. The moment is the product of the weight of the load and the distance between the point of application of load and the hinge.

4 Results and Discussions

After defining material, force magnitude, force direction, and fixtures, an iterative solver is used to solve the mathematical model and provides the related results. The blue and red colors depict the variation limit of stress concentration and deformation around the critical points in the submodule. The variation in equivalent von Mises stress for the forearm link with the wrist handle is shown in Fig. 9a, with a maximum value of 41.92 MPa. Higher stress concentration is observed near the bolts, shafts, and hinges. The maximum stress values are much less than the yield limit of 270 MPa for aluminium alloy and 370 MPa for mild steel. The respective deformations observed are illustrated in Fig. 9b, with a maximum value of 0.631 mm at the tip of the forearm link. The magnitude of deformation decreases while moving away from the point of application of load.

After applying force and fixtures as boundary conditions on the rear arm link as shown in Fig. 5a, the mathematical model is solved using the default solver, i.e., power-based iterative conjugate gradient (P-ICG) solver. The rear arm link design is not complex and the stress induced due to applied forces is within the elastic limit of the material used and hence default solver works effectively in this case. As shown in Fig. 10a, the maximum value of von Mises stress is observed as 33.867 MPa near the shafts due to high-stress concentration. The maximum stress values generated are much less than the yield limit of 270 MPa of aluminium alloy. Reaction forces are

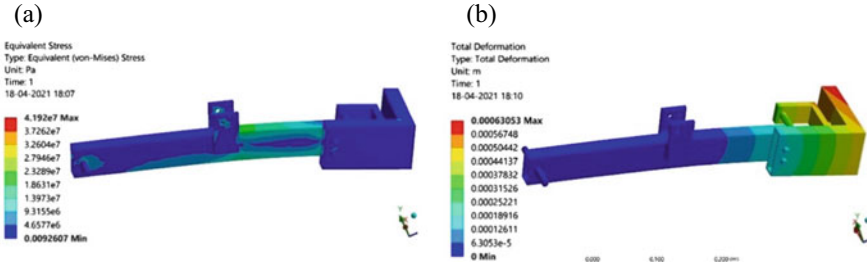


Fig. 9 Static structural analysis of forearm link **a** Equivalent von Mises stress; **b** Total deformation

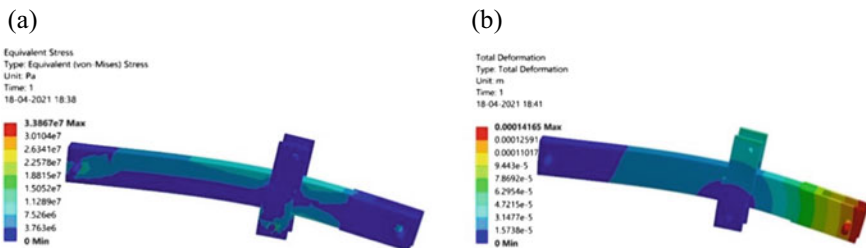


Fig. 10 Static structural analysis of rear arm link **a** Equivalent von Mises stress; **b** Total deformation

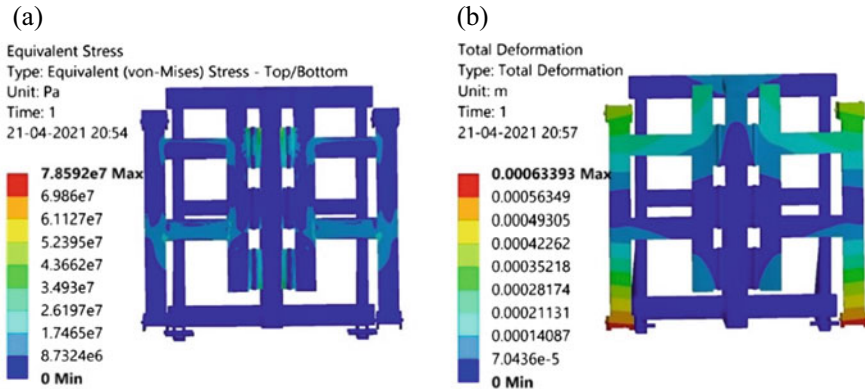


Fig. 11 Static structural analysis of double H-frame along with back frame **a** Equivalent von Mises stress; **b** Total deformation

responsible for deformation in the rear arm. Maximum deformation of 0.14165 mm is observed near the point where reaction forces act (shown as red color in Fig. 10b).

The reaction forces are calculated and applied to perform static-structural analysis on the double H-frame and back frame, as shown in Fig. 6b. Thereafter, shafts are fixed at the hip joint as a boundary condition, and an iterative solver is used to solve the mathematical model. The variation in generated von Mises stress is shown in Fig. 11a, with a maximum value of 78.592 MPa. All the forces from arm assembly are transferred to the H-frames, which are connected to the back frame through hinges. Hinges are bolted to the back frame and do not allow motion in the perpendicular direction; however, the moment due to the lifted weight tends to rotate the H-frames, which eventually rotate the hinges in the restricted direction. Therefore, the restriction of motion generates a significant value of the reaction couple, which leads to a high-stress concentration near that region. The maximum stress values generated are much less than the yield limit of 270 MPa of the aluminium alloy. Figure 11b shows the deformation in the H-frames with a maximum value of 0.63393 mm.

After applying forces with the fixed constraints, the results for the equivalent von Mises stress are presented in Figs. 12a and 13a. The corresponding results for total deformation are illustrated in Figs. 12b and 13b. It is essential to be noted that the total deformation represents the movement of the assembly in a specific direction instead of deformation within the parts. In the first case (when feet are in ground contact), the maximum stress is 140.62 MPa on the extreme side of the right hip due to localized bending of the straight beam, and the minimum stress is 0.034 Pa on the left foot as most of the stress is distributed in the system above feet. For the second case (when the left leg is swinging in the air), the maximum stress of 189.9 MPa is observed at the ankle joint of the right leg due to the maximum transfer of load on only one leg, which increases the compression force. The minimum stress of 0.039 Pa

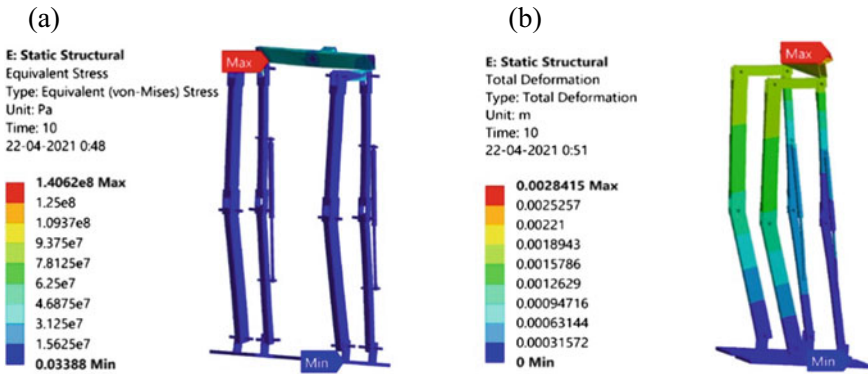


Fig. 12 Static structural analysis of leg links when both foot ground contact **a** Equivalent von Mises stress; **b** Total deformation

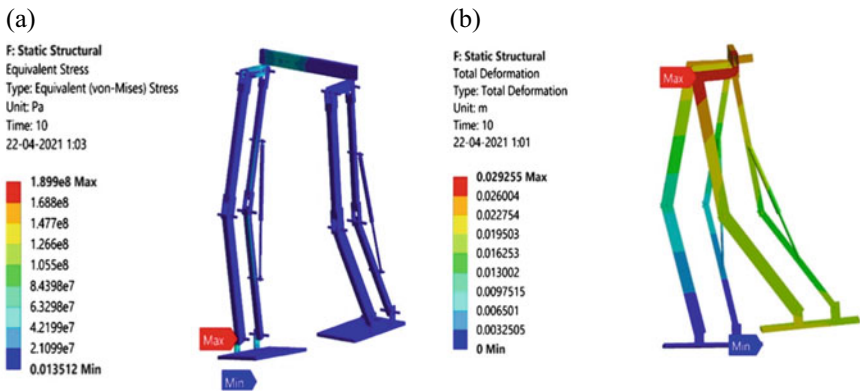


Fig. 13 Static structural analysis of leg links when left swinging in the air **a** Equivalent von Mises stress; **b** Total deformation

is observed on both feet. All the stress values observed in the system are within the yield limit of 270 MPa of aluminium alloy and do not lead to any failure.

Table 3 lists the maximum equivalent stress and maximum deformation in the critical parts in both conditions. The maximum deformation in the first case is observed as 2.84 mm on the hip in the upward direction. This deformation varies depending upon the subject’s weight, which is currently not considered in this work. For the second case, the maximum deformation of 29.2 mm is observed on the left extreme of the hip in the downward direction. Here, the forces due to load and moment of load try to push down the swinging leg back to the ground. In the actual scenario, the subject wearing the suit can easily control this movement by applying force in the opposite direction. From Table 3, it is to be noted that the deformation values in the second case for leg links and joints are more significant in magnitude; however, they

Table 3 Maximum equivalent von mises stress and maximum deformation in leg links and joints (First case: both foot on the ground; second case: left leg swinging in the air)

Cases	Component stress (MPa) and deformation (mm)	Thigh link	Calf link	Hip joint	Knee joint	Ankle joint
First case	Max. von Mises stress	$3 \times 10^{-}$	31.25	140.62	31.25	15.625
	Max. deformation	2.21	0.9	2.84	1.11	0
Second case	Max. von Mises stress	21.09	21.09	126.8	58.42	189.9
	Max. deformation	29.2	16.52	29.2	19.53	19.53

do not represent the deformation within the links. Furthermore, all the maximum values are observed for the left leg links. This is due to the suspended link in the air trying to lower down with no support attached. Support, in real scenarios, is provided by the subject who wears it. Therefore, all the deformations in the system are within safe limits.

The database, as mentioned above, is obtained after the simulation (stage 4) in ANSYS static-structural workbench. The database contains the plots of stress, plots of deformation, maximum and minimum von Mises stresses, and maximum and minimum deformation values. The simulation results suggest that the aluminium alloy can withstand the stresses generated in the exoskeleton due to the loading. Thus, the analysis suggests that all the critical components are safe during these extreme loading conditions and no further design changes are required. Moreover, these results can be used to reference future development of exoskeleton devices, which may include more lightweight and high-yield strength materials like carbon fiber, functional composites, etc. The holes for joints and the hinges at the back frame have high-stress concentration, suggesting use of high-yield strength components like bearings. High-stress concentration near the hip and ankle joint indicates the provision of fillets at the right angles.

5 Conclusions

In this work, a novel design of a full body exoskeleton has been presented along with the FEA analysis. Primarily, a stage-wise design methodology has been presented to develop the practical exoskeletons following the literature. Thereafter, the novel design of a 12-DOFs full body exoskeleton device for load augmentation has been proposed, and related modules have been explained extensively. Finite element analysis (FEA) in ANSYS static-structural workbench has been performed for the critical submodules subjected to maximum loads. The generated maximum von Mises stress and deformation have been computed for different upper body and lower body submodules. All the stresses have been found to be less than the yield limit of assigned

materials, and have not shown the failure of any functional part. Moreover, the deformations have been observed within the safe limits, which concludes that the structure can safely lift 25 kg in static condition and 15 kg in dynamic condition. In future, more work can be carried out to increase the DOF of the suit to provide comfort to the user. Moreover, the design can be improved to become more ergonomic for better comfort to the user. The dynamic analysis of the design can be performed for acquiring reliable results in dynamic conditions.

References

- Chen F, Yu Y, Ge Y, Sun J, Deng X (2007) WPAL for enhancing human strength and endurance during walking. In: 2007 international conference on information acquisition. IEEE, Seogwipo, South Korea, pp 487–491
- Christensen S, Bai S, Rafique S, Isaksson M, O’Sullivan L, Power V, Virk GS (2018) AXO-SUIT-A modular full-body exoskeleton for physical assistance. In: IFToMM symposium on mechanism design for robotics. Springer, Cham, pp 443–450
- Dhand S, Singla A, Virk GS (2016) A brief review on human-powered lower-limb exoskeletons. In: Conference on mechanical engineering and technology (COMET-2016), IIT (BHU). Varanasi, India, pp 116–122
- eksobIONICS. <https://eksobionics.com/eksoworks/>. Last accessed 26 May 2021
- Fontana M, Verthey R, Marcheschi S, Salsedo F, Bergamasco M (2014) The body extender: a full-body exoskeleton for the transport and handling of heavy loads. *IEEE Robot Autom Mag* 21(4):34–44
- Gorgey AS (2018) Robotic exoskeletons: The current pros and cons. *World J Orthopedics* 9(9):112
- Gorgey AS, Sumrell R, Goetz LL (2019) Exoskeletal assisted rehabilitation after spinal cord injury. *Atlas Orthoses Assist Devices* 440–447
- Hosseini M, Meattini R, Palli G, Melchiorri C (2017) A wearable robotic device based on twisted string actuation for rehabilitation and assistive applications. *J Robot*
- Junius K, Degelaen M, Lefeber N, Swinnen E, Vanderborght B, Lefeber D (2017) Bilateral, misalignment-compensating, full-DOF hip exoskeleton: design and kinematic validation. *Appl Bionics Biomech*
- Kalita B, Narayan J, Dwivedy SK (2020) Development of active lower limb robotic-based orthosis and exoskeleton devices: a systematic review. *Int J Social Robot* 1–19
- Karlin S (2011) Raiding iron man’s closet [Geek life]. *IEEE Spectr* 48(8):25–25
- Kazerooni H, Guo J (1993) Human extenders. *ASME J Dyn Syst Meas Control* 115(2(B))
- Kiguchi K, Iwami K, Yasuda M, Watanabe K, Fukuda T (2003) An exoskeletal robot for human shoulder joint motion assist. *IEEE/ASME Trans Mechatron* 8(1):125135
- Kim S, Nussbaum MA, Esfahani MIM, Alemi MM, Alabdulkarim S, Rashedi E (2018) Assessing the influence of a passive, upper extremity exoskeletal vest for tasks requiring arm elevation: Part I—“Expected” effects on discomfort, shoulder muscle activity, and work task performance. *Appl Ergon* 70:315–322
- Kong K, Jeon D (2006) Design and control of an exoskeleton for the elderly and patients. *IEEE/ASME Trans Mechatron* 11(4):428–432
- Kung PC, Ju MS, Lin CCK (2007) Design of a forearm rehabilitation robot. In: 10th international conference on rehabilitation robotics. IEEE, Noordwijk, Netherlands, pp 228–233
- Martinez F, Retolaza I, Lecue E, Basurko J, Landaluze J (2007) Preliminary design of an upper limb IAD (Intelligent Assist Device). In: Challenges for assistive technology. IOS Press, pp 530–534
- Mattsson P, O’Sullivan L, Power V (2018) Development and testing of full-body exoskeleton AXO-SUIT for physical assistance of the elderly. In: *Wearable robotics: challenges and trends:*

- proceedings of the 4th international symposium on wearable robotics, WeRob2018, Vol 22. Springer, Pisa, Italy, p 180
- Mori Y, Okada J, Takayama K (2006) Development of a standing style transfer system “ABLE” for disabled lower limbs. *IEEE/ASME Trans Mechatron* 11(4):372380
- Narayan J, Kalita B, Dwivedy SK (2021) Development of robot-based upper limb devices for rehabilitation purposes: a systematic review. *Augment Hum Res* 6(1):1–33
- Narayan J, Kumar Dwivedy S (2021) Preliminary design and development of a low-cost lower-limb exoskeleton system for paediatric rehabilitation. *Proc Inst Mech Eng Part H: J Eng Med* 235(5):530–545
- Narayan J, Jhunjhunwala S, Gupta M, Dwivedy SK (2020) Backpropagation neural network based design of a novel sit-to-stand exoskeleton at seat-off position for paraplegic children. In: 6th international conference on control, automation and robotics (ICCAR). IEEE, Singapore, pp 546–552
- Nilsson M, Ingvast J, Wikander J, von Holst H (2012) The soft extra muscle system for improving the grasping capability in neurological rehabilitation. In: 2012 IEEE-EMBS conference on biomedical engineering and sciences. IEEE, Langkawi, Malaysia, pp 412–417
- Pang Z, Wang T, Yu J, Liu S, Zhang X, Jiang D (2020) Design and analysis of a flexible, elastic, and rope-driven parallel mechanism for wrist rehabilitation. *Appl Bionics Biomech*
- Pedrocchi A, Ferrante S, Ambrosini E, Gandolla M, Casellato C, Schauer T, Klauer C, Pascual J, Vidaurre C, Gföhler M, Reichenfeller W (2013) MUNDUS project: multimodal neuroprosthesis for daily upper limb support. *J Neuroeng Rehabil* 10(1):1–20
- Pratt JE, Krupp BT, Morse CJ, Collins SH (2004) The RoboKnee: an exoskeleton for enhancing strength and endurance during walking. In: IEEE international conference on robotics and automation, 2004. Proceedings. ICRA'04. vol 3. IEEE, New Orleans, LA, pp 2430–2435
- Rahman MH, Kittel-Ouimet T, Saad M, Kenné JP, Archambault PS (2012) Development and control of a robotic exoskeleton for shoulder, elbow and forearm movement assistance. *Appl Bionics Biomech* 9(3):275–292
- Ratti N, Pilling K (1997) Back pain in the workplace. *Br J Rheumatol* 36(2):260–264
- Rubin J, Chisnell D (2008) Handbook of usability testing: how to plan, design and conduct effective tests. Wiley, New York
- Sankai Y (2010) HAL: Hybrid assistive limb based on cybernics. In: Kaneko M, Nakamura Y (eds) Robotics research. Springer tracts in advanced robotics, vol 66. Springer, Berlin, Heidelberg
- Seo K, Lee J, Park YJ (2017) Autonomous hip exoskeleton saves metabolic cost of walking uphill. In: 2017 international conference on rehabilitation robotics (ICORR). IEEE, London, UK, pp 246–251
- Suit X, MAX (Modular Agile eXoskeleton), <https://www.suitx.com/shoulderx>. Last accessed 26 May 2021
- Tagliamonte NL, Sergi F, Carpino G, Accoto D, Guglielmelli E (2013) Human-robot interaction tests on a novel robot for gait assistance. In: 2013 IEEE 13th international conference on rehabilitation robotics (ICORR). IEEE, Seattle, WA, USA, pp 1–6
- Toxiri S, Koopman AS, Lazzaroni M, Ortiz J, Power V, de Looze MP, O’Sullivan L, Caldwell DG (2018) Rationale, implementation and evaluation of assistive strategies for an active back-support exoskeleton. *Front Robot AI* 5:53
- Walsh CJ, Endo K, Herr H (2007) A quasi-passive leg exoskeleton for load-carrying augmentation. *Int J Humanoid Rob* 4(03):487–506
- Yan H, Wang H, Chen P, Niu J, Ning Y, Li S, Wang X (2021) Configuration design of an upper limb rehabilitation robot with a generalized shoulder joint. *Appl Sci* 11(5):2080
- Zaïri F, Moulart M, Fontaine C, Zaïri F, Tiffreau V, Logier R (2021) Relevance of a novel external dynamic distraction device for treating back pain. *Proc Inst Mech Eng Part H: J Eng Med* 235(3):264–272
- Zoss AB, Kazerooni H, Chu A (2006) Biomechanical design of the Berkeley lower extremity exoskeleton (BLEEX). *IEEE/ASME Trans Mechatron* 11(2):128–138